Matthias Zschornak[1,2] / Falk Meutzner[1,3] / Jessica Lück[4,5] / Arnulf Latz[4,5,6] / Tilmann Leisegang[1,3] / Juliane Hanzig[1] / Melanie Nentwich[1] / Jens Zosel[7] / Perla B. Balbuena[8]

Fundamental principles of battery design

[1] TU Bergakademie Freiberg (TUBAF), Institute of Experimental Physics, Leipziger Straße 23, Freiberg 09596, Germany, E-mail: matthias.zschornak@physik.tu-freiberg.de, falk.meutzner@physik.tu-freiberg.de, tilmann.leisegang@physik.tu-freiberg.de, juliane.hanzig@physik.tu-freiberg.de, melanie.nentwich@physik.tu-freiberg.de
[2] Helmholtz-Zentrum Dresden-Rossendorf e.V. (HZDR), Institute of Ion Beam Physics & Materials Research, Bautzner Landstraße 400, Dresden 01328, Germany, E-mail: matthias.zschornak@physik.tu-freiberg.de
[3] Samara National Research University (SNRU), Moskovskoye Shosse 34, Samara 443086, Russia, E-mail: falk.meutzner@physik.tu-freiberg.de, tilmann.leisegang@physik.tu-freiberg.de
[4] German Aerospace Center (DLR), Institute of Engineering Thermodynamics, Pfaffenwaldring 38-40, Stuttgart 70569, Germany, E-mail: jessica.lueck@dlr.de, arnulf.latz@dlr.de
[5] Helmholtz Institute Ulm (HIU) for Electrochemical Energy Storage, Helmholtzstraße 11, 89081 Ulm, Germany, E-mail: jessica.lueck@dlr.de, arnulf.latz@dlr.de
[6] University of Ulm, Institute of Electrochemistry, Albert-Einstein-Allee 47, 89081 Ulm, Germany, E-mail: arnulf.latz@dlr.de
[7] Kurt-Schwabe-Institut für Mess- und Sensortechnik e.V. Meinsberg (KSI), Kurt-Schwabe-Str. 4, Waldheim 04736, Germany, E-mail: zosel@ksi-meinsberg.de
[8] Texas A&M University, Artie McFerrin Department of Chemical Engineering, 100 Spence St, TX 77843 College Station, United States of America, E-mail: balbuena@mail.che.tamu.edu

Abstract:
With an increasing diversity of electrical energy sources, in particular with respect to the pool of renewable energies, and a growing complexity of electrical energy usage, the need for storage solutions to counterbalance the discrepancy of demand and offer is inevitable. In principle, a battery seems to be a simple device since it just requires three basic components – two electrodes and an electrolyte – in contact with each other. However, only the control of the interplay of these components as well as their dynamics, in particular the chemical reactions, can yield a high-performance system. Moreover, specific aspects such as production costs, weight, material composition and morphology, material criticality, and production conditions, among many others, need to be fulfilled at the same time. They present some of the countless challenges, which make battery design a long-lasting, effortful task. This chapter gives an introduction to the fundamental concepts of batteries. The principles are exemplified for the basic Daniell cell followed by a review of Nernst equation, electrified interface reactions, and ionic transport. The focus is addressed to crystalline materials. A comprehensive discussion of crystal chemical and crystal physical peculiarities reflects favourable and unfavourable local structural aspects from a crystallographic view as well as considerations with respect to electronic structure and bonding. A brief classification of battery types concludes the chapter.

Keywords: battery, electrochemistry, ionic transport, diffusion, migration, interface kinetics, crystallography
DOI: 10.1515/psr-2017-0111

Electrical energy is generally considered as highest quality form of energy, since it can easily be converted into other forms such as mechanical, thermal, or radiation energy. The drawback of electrical energy is the *problem of its storage*. Conventional capacitors provide only limited energy density which is why storage in other forms is inevitable for most applications. The *conversion to chemical energy* is a very efficient way to increase energy density by orders of magnitude but, due to the dynamics of the involved chemical processes, at the cost of power density (see Figure 1). This principle is realised for example in *modern super- or ultracapacitors*. In the most usual case, the electrostatic capacitance arises from charge separation at the electrodes' interfaces with ions in the electrolyte shielding the external electric field, the so-called Helmholtz double layers. By adding fast electronic charge-transfer from additionally reacting adsorbed ions at the electrode, the capacitance can be augmented by this supplementary *electrochemical pseudocapacitance*. Nevertheless, the accompanied increase in energy density is limited predominantly by the saturated amount of adsorbate at the interface. One solution to overcome this constraint of a limited interface region is to realise the electronic charge transfer and accompanied change of oxidation states for a large volume as is provided by batteries.

Matthias Zschornak is the corresponding author.

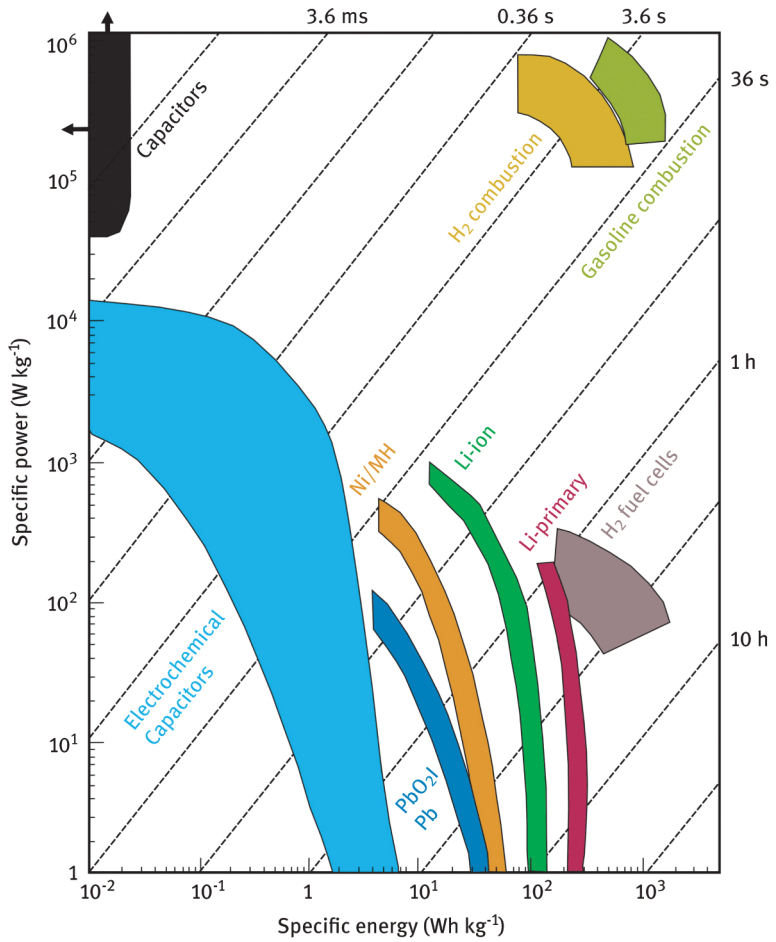

Figure 1: Ragone plot comparing specific energy and power of electrical and electrochemical energy storage technologies with conventional combustion technologies. Redrawn from [1] with additional data from [2].

Batteries contain electrochemical cells that convert the chemical energy stored in the active materials into electrical energy by means of ongoing exergonic electrochemical reactions. A cell is made up of two half-cells each consisting of an electronically conducting *electrode*, to deliver electric potential and current via contacts to an external circuit, and a volume of *electrolyte* interfacing the electrode. Both spatially apart half-cells are connected in series by a *separator* that prohibits electronic but permits ionic conduction in combination with the electrolyte to balance the disproportion of charge and to close the charge circuit. A schematic setup of a basic cell, the so-called Daniell cell (see section *The Daniell cell* for details), is shown in Figure 2.

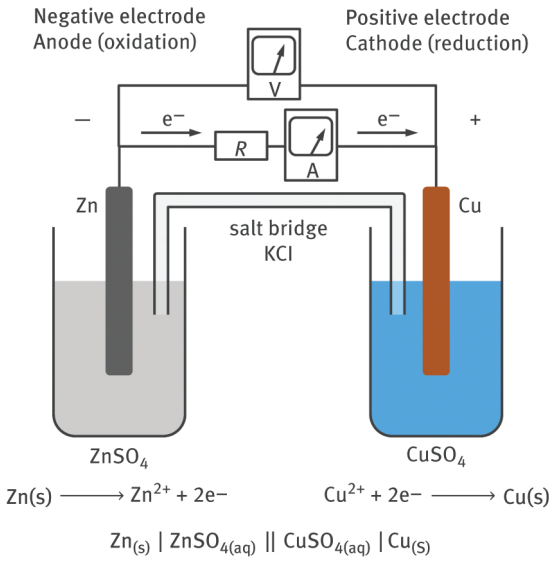

Figure 2: Daniell cell with oxidation of zinc at the anode and reduction of copper at the cathode. The cell voltage (V) will provide a current (A) for the outer electric circuit with resistance *R*.

The *oxidation* takes place in one half-cell increasing the oxidation state of the involved ionic species and depositing electrons into the respective electrode, the anode. During the discharge process, without externally applied electric potential, this electrode acquires a negative charge and corresponds to the electrode with the negative electric potential, also called negative mass. In the other half-cell, the *reduction* takes place decreasing the oxidation state of the participating ionic species and depleting the amount of electrons in the respective electrode, the cathode. During the discharge process, this electrode acquires a positive charge and corresponds to the electrode with the positive electric potential, also called positive mass. As the battery is being charged, an externally applied electric potential reverses ionic migration in the electrolyte and therefore anode and cathode and respectively the location of oxidation and reduction, but the negative and positive mass remain fixed. A more detailed description about these terms is given in chapter "Electrodes" of [3].

Nernst equation

The fundamental equation that relates the battery's cell potential to the concentration of reacting chemical species is the Nernst equation [4]. The charged battery is in a thermodynamically non-equilibrium state with an *excess of free enthalpy G* [J], also known as Gibbs free energy, i. e. chemically stored energy. This excess drives the chemical redox reaction towards the equilibrium state and is responsible for the electronic charge transfer with the electrodes and the accompanied electric potential providing the electric energy for the external circuit. The change in free enthalpy ΔG following the redox reaction induces a change in electrode potential ΔE [V] according to

$$\Delta G = -\nu_e e \Delta E$$

with ν_e being the electron transfer number for the reaction and e [C] the elementary charge. In the picture of a grand-canonical ensemble, i. e. systems with boundaries open to energy as well as particle transfer, ΔG is directly related to the chemical potential and can be derived from Boltzmann factors with Boltzmann constant k [J K^{-1}] respecting the probability for the ions to be in the oxidised or reduced state. The *Nernst equation*

$$\Delta E = \Delta E^0 + \frac{kT}{\nu_e e} \ln \frac{a_{\mathrm{Ox}}}{a_{\mathrm{Red}}},$$

named after the German physicist and chemist Walter Nernst, reflects this balance with the logarithm of the reaction quotient as the ratio of chemical activities a_{Ox} and a_{Red} for the oxidised and reduced form of the relevant ionic species, respectively. Since potential differences can only be measured as a voltage between two electrodes and the theoretical normalisation with respect to the vacuum energy is less accurate than relative voltage measurements, the standard hydrogen electrode H^+/H_2 is taken as a reference and assumed to be at 0 V for all temperatures T [K]. For standard ambient conditions (IUPAC-SATP), i. e. at T = 298.15K, a pressure p = 101.325 kPa, a concentration c = 1 mol/l with activity a = 1, and pH = 0, the respective *standard reduction electrode potentials* E^0 of common redox pairs are given in the electrochemical series. To present an overview, Table 1 summarises typical electrode potentials ranging from about −3 to +3 V. The full cell voltage results in $\Delta E^0 = E^0_{\mathrm{Red}} - E^0_{\mathrm{Ox}}$.

Table 1: Electrochemical series of common redox pairs.

Oxidised form	ν_e	Reduced form	E^0 (V)	References	Oxidised form	ν_e	Reduced form	E^0 (V)	References
Li^+	1	Li	−3.05	[5]	AgBr	1	Ag + Br^-	0.07	[5]
Rb^+	1	Rb	−2.93	[5]	Sn^{4+}	2	Sn^{2+}	0.15	[5, 6]
K^+	1	K	−2.93	[5]	Cu^{2+}	1	Cu^+	0.16	[5]
Ra^{2+}	2	Ra	−2.92	[5]	Bi^{3+}	3	Bi	0.20	[5]
Cs^+	1	Cs	−2.92	[5]	AgCl	1	Ag + Cl^-	0.22	[5]
Ba^{2+}	2	Ba	−2.91	[5]	Hg_2Cl_2	2	2Hg + 2Cl^-	0.27	[5]
Sr^{2+}	2	Sr	−2.89	[5]	Cu^{2+}	2	Cu	0.34	[5–8]
Ca^{2+}	2	Ca	−2.87	[5, 6]	ClO_4^- + H_2O	1	ClO_3^- + 2OH^-	0.36	[5]
Na^+	1	Na	−2.71	[5, 6]	Cu^+	1	Cu	0.52	[5, 6]

La^{3+}	3	La	−2.52	[5]	I_3^-	2	$3I^-$	0.53	[5]
Cd^{3+}	3	Ce	−2.48	[5]	I_2	2	$2I^-$	0.54	[5, 6]
Mg^{2+}	2	Mg	−2.36	[5, 6]	MnO_4^-	1	MnO_4^-	0.56	[5]
Sc^{3+}	3	Sc	−2.09	[5]	MnO_4^{2-} + $2H_2O$	2	MnO_2 + $4OH^-$	0.60	[5]
U^{3+}	3	U	−1.79	[5]	Hg_2SO_4	2	2Hg + SO_4^{2-}	0.62	[5]
Al^{3+}	3	Al	−1.66	[5]	BrO^- + H_2O	2	Br^- + $2OH^-$	0.76	[5]
Ti^{2+}	2	Ti	−1.63	[5]	Fe^{3+}	1	Fe^{2+}	0.77	[5, 6]
V^{2+}	2	V	−1.19	[5]	Hg_2^{2+}	2	2Hg	0.79	[5]
Mn^{2+}	2	Mn	−1.18	[5]	NO_3^- + $2H^+$	1	NO_2 + H_2O	0.80	[5]
Cr^{2+}	2	Cr	−0.91	[5]	Ag^+	1	Ag	0.80	[5, 6, 8]
$2H_2O$	2	H_2 + $2OH^-$	−0.83	[5]	Hg^{2+}	2	Hg	0.86	[5]
$Cd(OH)_2$	2	Cd + $2OH^-$	−0.81	[5]	ClO^- + H_2O	2	Cl^- + $2OH^-$	0.89	[5]
Zn^{2+}	2	Zn	−0.76	[5, 6, 8]	$2Hg^{2+}$	2	Hg_2^{2+}	0.92	[5]
Cr^{3+}	3	Cr	−0.74	[5, 6]	NO_3^- + $4H^+$	3	NO + $2H_2O$	0.96	[5, 6]
U^{4+}	1	U^{3+}	−0.61	[5]	Pu^{4+}	1	Pu^{3+}	0.97	[5]
In^{3+}	1	In^{2+}	−0.49	[5]	Br_2	2	$2Br^-$	1.09	[5]
S	2	S^{2-}	−0.48	[5, 6]	$O_2 + 4H^+$	4	$2H_2O$	1.23	[5, 6]
Fe^{2+}	2	Fe	−0.44	[5]	ClO_4^- + $2H^+$	2	ClO_3^- + H_2O	1.23	[5]
In^{3+}	2	In^+	−0.44	[5]	MnO_2 + $4H^+$	2	Mn^{2+} + $2H_2O$	1.23	[5]
Cr^{3+}	1	Cr^{2+}	−0.41	[5]	O_3 + H_2O	2	O_2 + $2OH^-$	1.24	[5, 7]
Cd^{2+}	2	Cd	−0.40	[5, 6]	$Cr_2O_7^{2-}$ + $14H^+$	6	$2Cr^{3+}$ + $7H_2O$	1.33	[5, 6, 9]
In^{2+}	1	In^+	−0.40	[5]	Cl_2	2	$2Cl^-$	1.36	[5, 6]
Ti^{3+}	1	Ti^{2+}	−0.37	[5]	Au^{3+}	3	Au	1.40	[5]
$PbSO_4$	2	Pb + SO_4^{2-}	−0.36	[5]	MnO_4^- + $8H^+$	5	Mn^{2+} + $4H_2O$	1.51	[5, 6, 9]
In^{3+}	3	In	−0.34	[5]	Mn^{3+}	1	Mn^{2+}	1.51	[5]
Tl^+	1	Tl	−0.34	[5]	2HBrO + $2H^+$	2	Br_2 + $2H_2O$	1.60	[5]
Co^{2+}	2	Co	−0.28	[5, 6]	Ce^{4+}	1	Ce^{3+}	1.61	[5]
Ni^{2+}	2	Ni	−0.23	[5, 7]	2HClO + $2H^+$	2	Cl_2 + $2H_2O$	1.63	[5]
AgI	1	Ag + I^-	−0.15	[5]	Pb^{4+}	2	Pb^{2+}	1.67	[5]
In^+	1	In	−0.14	[5]	Au^+	1	Au	1.69	[5]
Sn^{2+}	2	Sn	−0.14	[5, 6]	H_2O_2 + $2H^+$	2	$2H_2O$	1.78	[5]
Pb^{2+}	2	Pb	−0.13	[5, 6]	Co^{3+}	1	Co^{2+}	1.81	[5]
O_2 + H_2O	2	HO_2^- + OH^- −	−0.08	[5]	Ag^{2+}	1	Ag^+	1.98	[5]
Fe^{3+}	3	Fe	−0.04	[5]	$S_2O_8^{2-}$	2	$2SO_4^{2-}$	2.05	[5]
Ti^{4+}	1	Ti^{3+}	0.00	[5]	$O_3 + 2H^+$	2	O_2 + H_2O	2.07	[5–7]
H^+	2	H_2	0.00	[5–9]	F_2	2	$2F^-$	2.87	[5–7, 9]

The Daniell cell

The Daniell cell is considered the first electrochemical cell able to deliver current for a long time. It was invented by John F. Daniell in 1836 and is based on the observations of Luigi Galvani in 1786 on frog legs and Alessandro Volta's pile of alternating copper and zinc discs in 1800, which is considered the very first "wet battery cell" [10].

A Daniell cell consists of a zinc and a copper electrode immersed in zinc sulfate and copper(II) sulfate electrolyte solutions, respectively. Considering the metal electrodes, zinc is less noble than copper with a work function of 4.34 eV [11] and 4.65 eV [7], respectively. Furthermore, Zn has a much higher solution pressure [12] causing a significantly higher concentration of Zn^{2+} in the zinc sulfate than Cu^{2+} in the copper(II) sulfate solution as well as a significantly higher concentration of electrons in the zinc than in the copper electrode. The metal ions in both electrolyte solutions will stay close to the metal electrode interfaces forming the *Helmholtz double layer*, with an accompanied charge separation that causes the electric potential difference between each electrode/electrolyte interface. The full cell as combination of both half-cells is driven by the oxidation of metallic zinc $Zn_{(s)}$ in the solid state (s) and the simultaneous reduction of copper(II) ions $Cu^{2+}_{(aq)}$ in solution (aq) (see Figure 2) according to

$$Zn_{(s)} \overset{+0.76\,V}{\rightarrow} Zn^{2+}_{(aq)} + 2e^-$$

$$Cu^{2+}_{(aq)} + 2e^- \overset{+0.35\,V}{\rightarrow} Cu_{(s)}$$

with standard electrode potentials $E^0_{Zn^{2+}/Zn} = -0.76\,V$ and $E^0_{Cu^{2+}/Cu} = +0.35\,V$ providing a total electrode potential difference of +1.11 V for the full redox reaction:

$$Zn_{(s)} + Cu^{2+}_{(aq)} \overset{+1.11\,V}{\rightarrow} Zn^{2+}_{(aq)} + Cu_{(s)}$$

As soon as the outer electronic circuit is closed, the redox potentials can act and supply electrical energy by means of the electrode potential difference and the used current. The ongoing reactions will accumulate positively charged Zn^{2+} ions in the electrolyte of the anode half-cell (referred to as anolyte) and SO_4^{2-} in the electrolyte of the cathode half-cell (referred to as catholyte) due to the depletion of Cu^{2+} ions. This imbalance of ionic charge between both electrolytes and the resulting electrostatic potential as well as the local excess of product (anode) and shortage of reactant (cathode) species would saturate the reactions at some point. To counter this saturation, a salt bridge (separator with electrolyte) connects the electrolytes of both half-cells. It is made up of a chemically inert salt with respect to the electrolytes, e. g. Na_2SO_4, possibly with similar conductivity of anions and cations. It allows SO_4^{2-} and Na^+ ions from the salt bridge to neutralise the Zn^{2+} and SO_4^{2-} excess, respectively. The concentration imbalance of the salt's remaining ions and the accompanied difference in chemical potential between the electrolyte/salt bridge interfaces will be reduced by ionic migration of predominantly Na^+ ions from the anode and SO_4^{2-} ions from the cathode half-cell through the bridge. The whole cell is a combined series of electrochemical gradients which induce mass and charge transport and determine the dynamics of the battery discharge process towards the equilibrium state. Specific electrochemical cells with a solid electrolyte will be discussed in detail in chapter "Separators and Solid Electrolytes" of [3].

Reactions at electrified interfaces

Regardless of the choice of system, electrochemical storage of energy is largely based on interfacial reaction and transport processes, which determine the overall performance. In principle, all electrochemical systems have at least two chemically different but conducting phases. At the phase boundary, free charge carriers are rearranged due to different properties of the phases. Thus, the interface is electrified and local electric fields are produced. Those formed space charges and potential gradients affect reactions at or across phase boundaries. For electrochemical systems with a solid electrode and a liquid electrolyte, the charged region at the interface is called *electrochemical double layer*. In the twentieth century, the conception of the electrochemical double layer was developed. With the work of Helmholtz [13] on charge distributions in conducting materials, the term *electrical double layer* was introduced for the formation of two oppositely charged layers at the surface. Including work done in the field of electrocapillarity of liquids [14, 15], a first double layer model regarding the metal–electrolyte interface was established by Chapman in 1913 [16]. Stern finalised the concept of the double-layer structure describing a fixed and a diffusive part of the charged layer in the liquid phase [17]. Because of this historical development, the electrochemical double layer is pictured as an inner and outer Helmholtz layer, which denotes specifically and nonspecifically adsorbed ions, and a diffuse or Gouy–Chapman layer in the electrolyte, see Figure 3. Based on this concept of the structure, the theory of the electrochemical double layer characterizing charges and electric potentials was extended by several aspects like e. g. dipole properties or volumetric effects [6, 18]. A summary of the theoretical models of the electrochemical double layer combined with the field of electrocapillarity can be found in the classical paper of Grahame [19].

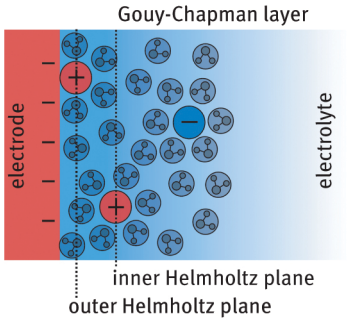

Figure 3: Schematic illustration of the electrochemical double layer formed at the electrode–electrolyte interface.

In parallel to this development, the reaction kinetics at the electrolyte–electrode interface were investigated. A general expression for the transfer rate of electrons was derived from kinetic theory for the case of hydrogen evolution and metal deposition [20–22]. This relation describing the solid electrode current density i_{se} [A m^{-2}] for an arbitrary charge transfer reaction is known as the Butler–Volmer equation

$$i_{se} = i_0 \left(\exp\left(\frac{\alpha_A e}{kT} \eta_s \right) - \exp\left(-\frac{\alpha_C e}{kT} \eta_s \right) \right),$$

where α_A and α_C with $\alpha_A + \alpha_C = 1$ are the weighting factors of the anodic and cathodic part of the reaction due to the overpotential η_s [V]. The exchange current density i_0 [A m^{-2}] depends on the composition of the reactants and products. The driving force of the reaction is given by the measured overpotential η_s, which describes the difference of electrochemical potential of reduced and oxidized state (further details given in chapter "Electrodes" of Ref. [3]). In Ref. [23], the Butler–Volmer equation was used for the first time to describe the intercalation reaction in a lithium ion battery. This has now become the standard approach for modelling electrode reaction kinetics in electrochemical systems. A first relation between the structure of the double layer and the reaction rate of the electrode was found by Frumkin [24]. Here, the overvoltage of a metal deposition reaction was deduced by considering the potential distribution in the double layer. Further developments lead to the generalised Frumkin–Butler–Volmer equation [25], which adapts the classical Butler–Volmer relation to capacitive processes of the double layer. The general form of the Butler–Volmer equation is preserved; however, effective transfer coefficients α^* including the structure of the double layer are introduced. This corresponds to a charge free layer between electrode and diffuse double layer, namely the Stern layer, and an electron transfer at the outer Helmholtz plane, which depends on the thickness of the Stern layer. As a result, one implicitly neglects ion adsorption on the inner Helmholtz plane and a dynamic behaviour of the double layer.

Approaches have been made to strengthen the connection of the Butler–Volmer equation to electrochemical systems. Derivations based on concepts of non-equilibrium thermodynamics were presented [26, 27]. Electron transfer reactions, where no breaking or establishing of chemical bonds occur, can also be expressed in similar terms [28]. Furthermore, a sequential treatment of an electrode reaction is possible by considering ion adsorption and space charges at an electrified interface [29]. Nevertheless, an accurate description of reaction kinetics at electrochemical interfaces is still a challenging task for today's research. It presents an indispensable element of any physics-based model of electrochemical systems, which is a necessary tool for improving battery design and performance.

Diffusion and migration in crystals

As already indicated above, electrochemical energy storage is based on the movement and valence state change of ionic species in matter. Therefore, the most important atomic processes involved in these reactions comprise the diffusion or, in terms of an electric field driven process, the migration of charged ions through a liquid or solid matrix. Both processes strongly depend on the type of electrolyte and electrochemical redox reaction. The electrolyte is especially important for the kinetics providing ionic and preventing electronic migration, as it may and in case of solid electrolytes often does present the limiting transport rates and thus the electric power capabilities of the device. The redox reaction describes the participating redox couples and available electrons per reaction and determines, apart from overpotential losses, the potential differences or respective voltage of the cell and as a consequence the highest achievable theoretical energy density. Both factors are of tremendous importance for electrochemical energy storage since they eventually define the field of application and the impact of a certain chemistry within the respective field.

Diffusion is a very general concept that is observed on very different scales and even different fields of science. Generally speaking, diffusion describes the movement of a "particle" due to a concentration gradient. In chemistry and physics, this phenomenon can be observed for example when a drop of coloured solute is added to a colourless solvent (see Figure 4(a)). If the mixture is not stirred, the solute will slowly start to colour the solvent, starting from the highly concentrated point where the drop was added. This process is driven by the different concentrations of solute in the solvent: solute particles move towards the regions of lowest solute concentration in order to equalise the concentration in the whole solvent. Similar concentration-driven redistribution of particles takes place in solids, as is exemplified in Figure 4(b) for atomic interdiffusion at metal/metal interfaces.

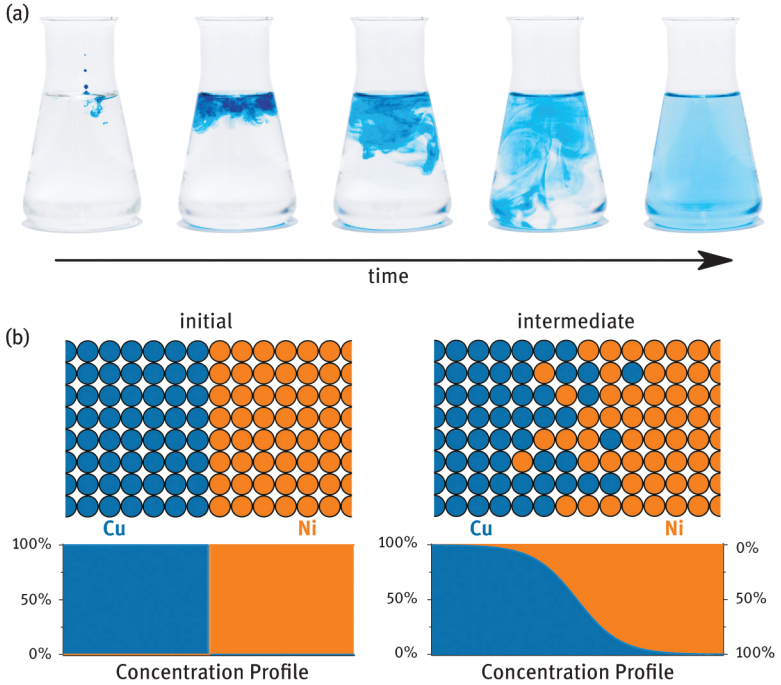

Figure 4: Diffusion of dye in a liquid (upper part). After an initially convection-dominated redistribution, the dye moves from highest to lowest concentration until it is evenly distributed throughout the liquid. [Photo by S. Jachalke]. Diffusion of atoms in a solid (lower part) illustrated at the interface of two phases with similar atomic structure but made up of different types of atoms Cu and Ni with a certain degree of solubility for the other type in each phase. With increasing time, the concentration step will smear out as atoms switch positions and move into the other phase.

Mathematically, based on continuity equation for a conserved number of particles, the particle diffusion flux j_D [m^{-2} s^{-1}] causes the change of particle density n [m^{-3}] with progressing time t [s] and is described by Fick's first and second law [30] and the general local relations

$$\nabla j_D = \nabla(-D \cdot \nabla n) = -\partial n/\partial t = -D\Delta n,$$

where D [m^2 s^{-1}] is the so-called diffusion coefficient that describes the magnitude of the process – the proportionality constant with respect to the density gradient. The higher the density gradient between two reservoirs, the faster will be the transport process.[1] This Laplacian relation reflects the local particle redistribution towards an equilibration distribution, i. e. a positive local curvature of the particle density will promote a local inward flux, whereas a negative curvature will cause an outward flux. In the picture of charge redistribution, it is convenient to include the elementary charge e [C] into the basic physical quantities, i. e. multiplying the above equation with particle charge q [C]. This way j_D becomes the diffusion current density J_D representing the flux of charge diffusion in [C m^{-2} s^{-1}] or [A m^{-2}] with $\rho = qn$ in [C m^{-3}] denoting the charge density.

Apart from a density gradient, charged atoms or ions can also move through arrangements of ions due to the application of an electric field. Similar to electrons, ions move along the electric field or respective electric potential $\pm\nabla\varphi$. When the gradient is inverted, the ions' movement will be inverted as well. This process is called ionic "conduction" or "migration" and thus also allows the directed movement of ions in absence of a density gradient and even against it, if the electromotive force[2] is high enough. Similarly to Fick's equation, conduction is described as

$$J_C = |\rho|\,\mu E = \sigma E = -\sigma \cdot \nabla\varphi,$$

where $\boldsymbol{J}_C$ [A m^{-2}] is the current density induced by the electric field $\boldsymbol{E}$ [V m^{-1}], μ [m^2 V^{-1} s^{-1}] is the mobility of the charge carrier, σ [S m^{-1} = Ω^{-1} m^{-1}] the conductivity, and φ [V] the electric potential. Since μ is positive by definition, the absolute value of charge density ρ has to be used to ensure a unidirectionality of current density J_C and electric field E.

The ionic transport process is a superposition of diffusion and migration and depends on two potentials: the chemical and the electric potential, in sum referred to as the electrochemical potential. The stronger will dominate the movement of ions resulting in a total current density

$$J = -D\nabla\rho - |\rho|\,\mu\nabla\varphi.$$

Conductivity is closely related to the diffusion coefficient and describes the magnitude of achievable movement of ions due to a varying local electric potential $\varphi(r)$. In a classical Boltzmann picture, the equilibrium distribution according to the particle's electrostatic energy $q\varphi$ follows for a given temperature T [K], the exponential relation $n \sim e^{-q\varphi/kT}$. The gradient of the particle density then yields $\nabla n = -qn/kT \cdot \nabla\varphi$. From this relation originates, at zero net flux $J_D + J_C = 0$ and absence of external electric fields, the Nernst-Einstein equation

$$D = \mu kT/|q|$$

which connects material parameters of diffusion and migration.

The above-given basics are valid for liquid and solid systems. The following discussion focusses on solid electrolytes and all-solid-state type batteries, in particular based on crystalline materials, since these systems have a prospering future (cf. chapter "Separators and Solid Electrolytes" of Ref. [3]).

Crystallographic, crystal chemical, and crystal physical peculiarities

This article presents the electrochemistry of batteries from a solid-state physics point of view. The following section covers ideas and considerations that originate from the ordered structure of crystals specifically reflecting the interdisciplinary field of crystallography[3] as a tool to give a non-standard but appropriate approach for describing this field of research and application.

Ions in crystals are coordinated by other oppositely charged ions. In order to move from one site to another, this coordination needs to be weakened, which requires energy. Since diffusion or migration is described as an atomic jump from one equilibrium structural site via an intermediate region, possibly an intermediate site, to an equivalent equilibrium structural site (see Figure 5), crystallography is a powerful tool for the analysis of conduction processes. These capabilities are predominantly based on the high potential for the elucidation of equilibrium structures and electron distributions, which coupled with theoretical techniques provide useful predictions of ionic conductivity. The derived parameters cover primarily the potential barrier E_B [J or eV] and, taking into account the particle density as well, the diffusion coefficient. On an atomic level, the moving ion needs to overcome this energetic barrier as it passes through the atomic environment of the minimum-energy pathway for conduction. This is a statistical, thermally activated process based on the dynamic movement of the migrating ions with a certain attempt frequency f_i [s^{-1}] to overcome the migration barrier. This barrier is biased by the gradient of the electric potential reducing or increasing the barrier by the electrostatic energy $\pm q\Delta\varphi_i/2$ for forward and backward current, with an electric potential difference $\Delta\varphi_i$ per jump along the path i and a rate of success given by a classical Boltzmann-factor (for details see e. g. Ref. [31]). The accompanied drift velocity $v_D = \mu E$ [ms^{-1}] in field direction for a specific migration path i with effectively moved distance s_i [m]

$$v_{D,i} = f_i \cdot s_i \cdot N_i \left[\exp\left(-\frac{E_B - q\Delta\varphi_i/2}{kT}\right) - \exp\left(-\frac{E_B + q\Delta\varphi_i/2}{kT}\right)\right]$$

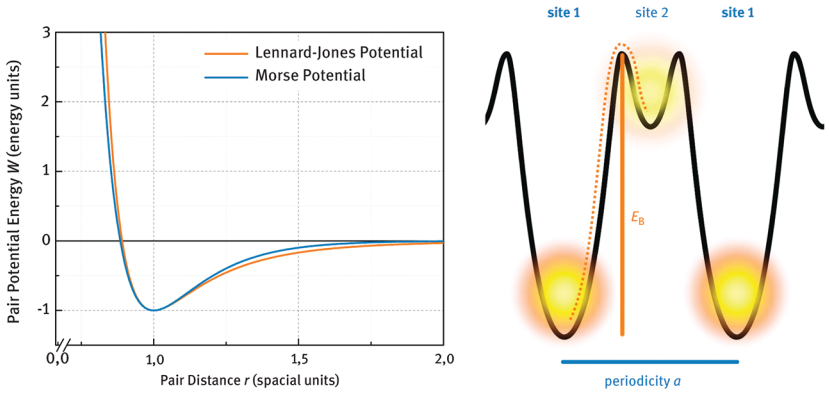

Figure 5: (a) Typical pair-interaction potentials of two atoms according to the Lennard–Jones and Morse potential type with a stable minimum position (here normalised to $r = 1$), a well depth (here normalised to $W = -1$) giving the dissociation energy and a certain well width defining strength and range of the bond. (b) Thermally activated hopping process illustrated for an atom on a stable site 1 via an intermediate site 2 to an equivalent stable site 1 in form of a double well potential with lattice periodicity a and migration barrier E_B.

depends further on the degeneracy[4] of the migration path N_i within the crystal structure of the ion conducting material. In crystalline materials, the drift velocity will depend on the crystallographic direction, with respect to path degeneracy, moved distance per successful jump, as well as barrier bias. Transport will preferentially take place in the vacancy or void network in between the discrete atomic positions, which are fixed by the crystal structure. Usually, cations present the most mobile species in solid-state batteries, although anions may be used as well [32].

The interatomic energy of an atom in the vicinity to another atom can be described by pair potentials, e. g. the Lennard–Jones potential, balancing out repulsive (due to the Pauli principle in case of overlapping orbitals) and attractive forces (e.g. van der Waals). Typically, three parameters are characteristic: the dissociation energy, an equilibrium bond distance, and the potential's well depth describing the range of the interaction (see Figure 5). The so-called Morse potential extends this description, taking into account anharmonicity of vibrational modes, the temperature dependence of the equilibrium distance, as well as the description of unbound states and bond breaking (see e. g. Ref. [5]). With respect to the equilibrium distance with another atom, pair potentials describe the increase in energy if the atom is displaced. Since the terms of attraction and repulsion between the coordinating atoms in summary depend on the geometrical arrangement and the direction into which the atom is displaced, there is always an energetically preferred path where migration proceeds.

The stronger the bonds between a moving cation and the surrounding anions, the more energy is required for the movement. In particular, ionic compounds may show the disadvantage of stronger, usually more isotropic interactions. Less electronegative elements – such as S instead of O, Cl instead of F – show better flexibility to electron density delocalisation and polarisability. The liquid-like density smooths the energy landscape of the migration path, in particular the discrete singularities of the ionic charge. These elements may form more directed, covalent bonds with other structure-constituting matrix-cations, which offer additional relaxational degrees of freedom during the hopping process. Preferentially, they are also less electron-affine so that they may compensate the electronegativity of the anions without altering the charge state of the moving cation as it approaches the bottleneck position. In general, decreasing changes in the interaction of the moving cation with the structural environment will flatten the energy landscape and decrease the energy barrier. These interactions are even stronger for higher valent ions, like Mg^{2+}, Ca^{2+}, Zn^{2+}, or Al^{3+}. Therefore, the local chemistry is extremely important for conductors of these cations.

A chemical concept regarding the possible bonding and bond strength of atoms and ions is called "HSAB" – theory of "hard" (strong) and "soft" acids and bases [33] – stating that strong acids form strong bonds with strong bases and weak bonds with soft bases. Analogously, soft acids and soft bases form strong bonds. The conduction channel in general provides an anionic environment, which is held together by matrix-cations. In order to have more independent conduction ions, the environment should mainly consist of anions with low affinity for a chemical bond to the moving ion and high affinity for bonding to the matrix-cations. Most of the (technologically) interesting cations for ionic conduction are "hard" acids. Therefore, matrices built from soft acids and bases are of particular interest [34]. In the case of Li, the S-containing ionic conductor materials identified to this point already show higher promise than their O-containing counterparts.

Ionic compounds mostly show isotropic, non-directional bonds, as each ion tries to surround itself by oppositely charged ions to passivate or shield central charge and minimise the energy of electric fields. This is best achieved in highly symmetric atomic environments and can be observed in many oxidic compounds, where metal-cations are in many cases tetrahedrally or octahedrally coordinated. These highly symmetric building blocks can then be constructed into crystal structures that may show very differing magnitudes of symmetry:

from highly symmetric cubic structures like spinels to completely amorphous silicates. Both of these extremes may show cations tetrahedrally coordinated by oxide ions [35].

"Classic crystallography" deals with 3D periodic structures that are described by a unit cell containing symmetry elements that leave the structure invariant. The more of these elements can be identified, the higher is the intrinsic symmetry of the system. In addition to the translation due to 3D periodicity, a high-symmetry structure presents multitudes of symmetry-equivalent regions and respective structure motives in a unit cell. For a structure of certain symmetry, from a crystallographic point of view, the lower the symmetry of a site,[5] the more symmetrically equivalent atoms are generated and the higher is this site's multiplicity. The set of symmetry-produced atoms of a specific atomic position is called crystallographic orbit, for which all atoms have an identical atomic environment and thus the same energy.

As described in Ref [36]., the most important chemical design principle for superionic conductors[6] is the presence of a plurality of partially occupied, energetically identical, or at least similar sites in the crystal structure. This principle is illustrated schematically in Figure 6. Multitudes of energetically identical sites can be identified in crystal structures by low-symmetry, high-multiplicity sites. In the best case, only one site of very high multiplicity is involved in the conduction process. The occupancy of this site is also an important factor in crystallography that is determined during the experimental crystal structure analysis. Of course, these sites have to be interconnected in order to allow the movement of an ion through the structure. The connectivity is defined by a percolation of conduction and intermediate sites. This means that at least one "infinite" path can be identified in the crystal structure, starting on a point of one face of a unit cell and arriving to this point, but on the exact opposite face of the unit cell or supercell. If this is not the case, a 0D path is formed (a loop). Infinite paths can be of 1D (tubes), 2D (planes), and 3D (networks) dimensionality (see Figure 7).

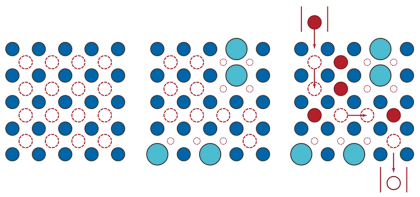

Figure 6: Graphic representation of the three main "crystallographic" features of a superionic conductor; in blue: matrix anions (matrix cations are omitted to avoid confusion), in red, dotted: void sites, in red, solid: conducted cations. A void network with void sites is needed for fast conduction. For a flat energy surface, energetically equivalent sites (left) are preferential, since larger or more displaced anions decrease the space and thus change the energy of the neighbouring voids (middle). For low energy sites within the conduction network – the dynamical traps, population of other void sites can be neglected in time-average – an occupancy of about one half is best, since each major hopping process can only be successful with an adjacent void. If the concentration is too low, the current is limited due to the migrating species. If it is too high, the current is limited due to the limited amount of necessary voids.

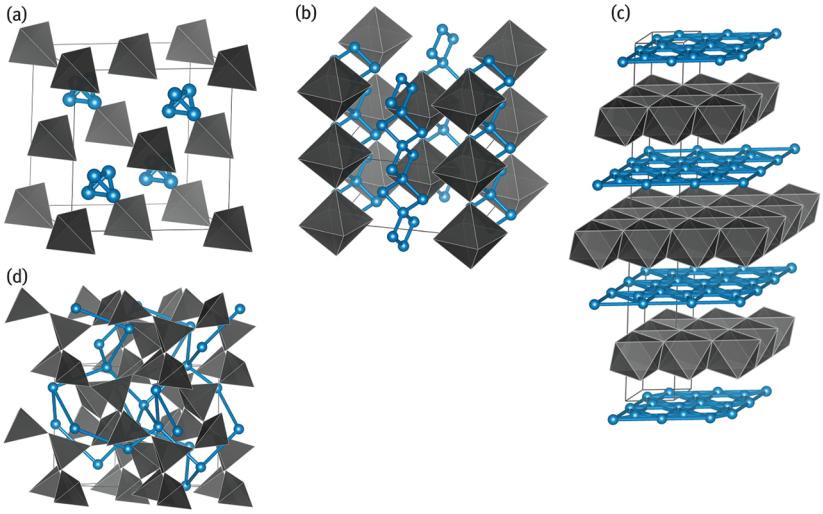

Figure 7: Basic matrix dimensionalities of an ion-conducting matrix (grey polyhedra) with highlighted conduction network (blue network): (a) 0D within a 3D conduction network, (b) 1D within a 1D conduction network, (c) 2D within a 2D conduction network, and (d) 3D within a 3D conduction network.

Crystal structures can be assigned to a crystal class because of their inherent symmetry. Because of Neumann's principle, which states that "if a crystal is invariant with respect to certain symmetry elements, any of

its physical properties must also be invariant with respect to the same symmetry elements" [37], certain dimensionalities can be expected: In cubic, only 3D paths are possible. If a conduction path is parallel to the designated axis (*c* axis) in hexagonal, trigonal, and tetragonal structure, it is at least 1D, if the path is perpendicular to the designated axis, it must be 2D. For all less symmetric crystal classes, no preferences can be deduced from the available symmetry operations.

Ideal candidates for good conduction are therefore highly symmetric structures. In the case of cationic transport, more accurately, a high-symmetry anion-sublattice should be aimed at [38]. High packing density anion networks exhibit multitudes of energetically identical or similar sites that are interconnected by likewise identical or similar coordination-polyhedra faces through which the movement between sites is mediated. In these cases, the channel between these sites consists of a triangle of anions that is penetrated by the moving cation. In a recent study, sulphur-containing Li^+-conductors were systematised according to their anion-package by comparing the anion-network to ideal packings of bcc, fcc, and hcp arrangements [34]. The highest promise was deduced from bcc arrangements of anions: the conduction sites are situated in tetrahedral sites which are directly connected to each other via a single jump from tetrahedron to tetrahedron. In fcc and hcp structures tetrahedral sites have no direct connection, they do not percolate, but an intermediate octahedral site needs to be passed. Additionally, there are no direct octahedron–octahedron connections. Therefore, two possibly energetically different sites increase the "complexity" of the migration network. In fact, the highest Li^+-conductivity sulphur-containing compounds show anion-arrangements that can be mapped to bcc.

In summary, the conduction network should show as little energetic deviation in the conduction path as possible. This is achieved by having percolating sites with more or less the same energy. Recently, it was also shown that this implication stays true even if only energetically unfavourable sites are occupied as long as this path is not connected to lower energy sites [39].

Crystallographic science along with X-ray diffraction, powder X-ray diffraction (PXRD), resonant X-ray diffraction (RXD), and neutron diffraction measurements provide excellent characterisations of structural features that are useful to infer ionic transport (details in chapter "Characterisation of battery materials" of Ref. [3]). PXRD in particular [40] is of relevance to identify porosity regions that could eventually become ionic conduction channels in solid state electrolytes or in solid conductors. In addition, RXD techniques provide spectroscopic sensitivities for the investigation of specific chemical species in the crystal structure, their valence states, crystallographic sites, as well as their respective structural phase [41, 42]. Once the crystal structure is characterised, first principles computational methods (discussed in chapter "Computational methods for battery material identification and analysis" of Ref. [3]) are extremely useful to identify minimum potential energy pathways for ions traveling the solid structures [43, 44] and diffusion mechanisms that can compete in a given solid or through solid/solid interfaces [45].

Classification of battery applications and types

Once adequate materials have been identified, the electrochemical cell, which is the smallest unit of a battery, may be designed. The general sequence of material layers is set by the respective electrochemistry, but the final form of the housing holding the cell may differ according to voltage, capacity, or space requirements of the application [46].

Small batteries, e. g. for consumer applications like flashlights, remote controls, etc., just consist of one electrochemical cell. Other applications like Laptop batteries require the connection of several cell units in parallel, in series, or both. Standards in cell packaging, e. g. of typical Li-ion batteries, comprise button, cylindrical, prismatic, and pouch cell geometries [47]. For the cylindrical battery, the material stack is cut to a specified width and rolled to the desired radius, whereas for the prismatic geometry the wrapping is flat, and for the pouch cell setup the flat material stacks are packed on top of each other to the desired height or are designed as prismatic flat wrap (see Figure 8). Prismatic cells can be packaged more efficiently than cylindrical cells because of their form factor and therefore the packing density is higher [9]. They are available in sizes up to 100 Ah, whereas sizes of up to 200 Ah are available for cylindrical cells. While cylindrical and prismatic cells are predominantly produced in hard cases, so-called pouch cells are mostly soft packs. They make the most efficient use of available space and achieve a packaging efficiency of 90–95 %. Because of the absence of a metal can, the pouch pack has a lower weight and therefore the battery pack will have a higher energy density. However, the cells have low mechanical stability and therefore a more robust packaging is required for many applications. Typically, several of these cells are connected to modules, which then contain also individual cell monitoring and temperature control. The assembly of individual modules eventually forms the final battery pack. All mentioned geometries are typically sealed with a metallic casing due to the impermeability for liquids, moisture, and air as well as for mechanical stability.

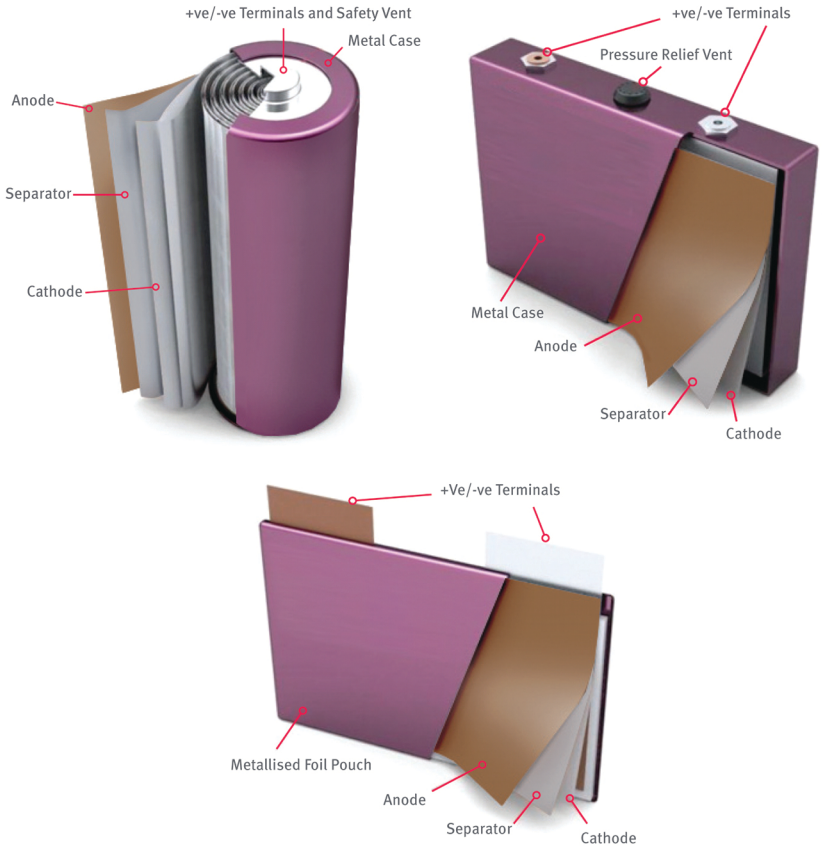

Figure 8: Standard geometries of conventional Li-ion batteries: cylindrical (upper left), prismatic (upper right), and pouch cell geometries (lower). Copyright Johnson Matthey Plc © 2012 [9] – reprinted with permissions.

In the case of commercially available Li-ion battery packs for automotive applications, about 500 single parts have to be assembled in one battery system, together with about 300 screw connections and 250 welding points [46]. The most widespread Li-ion battery on the market today is the 18,650 round cell. It has to be noted that for the emerging battery technologies, like the high-temperature Na–S battery, the cell design is different owing to the fact that the electrodes are liquid and therefore separated by a solid-state material. Hence, tube-shaped ceramics are used as containers here [48].

In today's life, batteries power numerous applications with diverse needs and demands for electrical energy in terms of parameters (voltage, energy density, current, power density, etc.) and handling (mobility, chargeability, cycle life, etc.). With respect to the powered device, one basic classification of a battery is therefore made according to its *portability. Mobile applications* comprise a variety of everyday consumer tools like mobile phones and smartphones, laptops, or watches up to electrically powered cars or busses, to name a few. *Stationary applications* may be used to balance generated and consumed electricity on all scales, from single houses to interregional or even national and international electrical grids, or to ensure power supply in case of grid failure, e. g. by means of uninterruptible power supplies. *Accessibility* as well as power demand often determine if a battery may be changed or recharged regularly or not, as is the case e. g. for medical applications like implantable neurostimulators or cardiac pacemakers, or batteries for military and space applications.

Batteries are further classified regarding their *chargeability. Primary* batteries are based on chemical reactions that cannot be easily reversed, which usually allows for higher energy densities. These batteries are disposed after use. *Secondary* batteries or accumulators can be recharged. They convert externally provided electrical energy back to chemically stored energy in the battery, reversing the internal chemical reactions. Thus, the battery can be cycled many times before degradation processes start to limit the capacity. *Tertiary* cells are sometimes referred to and describe cells with quasi-unlimited energy and power. They basically describe two electrodes that are independent of the active masses consumed during the electrochemical reactions. The more active mass is available, the more energy can be generated. Power can be increased by increasing the surface of the electrodes and thus the amount of charge generated per time. A fuel cell is the prime example for a tertiary cell, depending only on the amount of hydrogen and oxygen to be converted to water.

Battery types comprise various concepts to realise conversion of chemically stored energy to electrical energy. Among the most common, prevalent types are based on cation migration. Representatives cover, e. g., Li batteries [49], Ni–Cd batteries [50], polymer batteries [51], redox flow batteries [52–54], metal–air batteries [55],

Pb accumulators [56], and concentration cells [8]. Several of these types and concepts are presented in detail in chapter "Battery Concepts" of Ref. [3].

Notes

1 The model of heat flow uses the same kind of equation showing the generality of the concept.
2 Electromotive force is the voltage supplied to an electrical circuit by a source of electrical energy, such as a capacitor, a battery, or an electric generator.
3 Crystallography describes the atomic arrangement of crystalline matter and offers general tools for the description of non-periodic structures as well.
4 In the context presented here, the term degeneracy describes the number of symmetry-equivalent paths within the unit cell of the structure. The symmetry may be reduced by the specific direction of the electric field.
5 The International Union for Crystallography defines a symmetry operation as "a transformation under which two objects, or two configurations of an object, are brought to coincide" [57]. The crystallographic description of a structure is based on the placing of different symmetry elements – geometric elements, mostly points, lines, and planes, that apply a symmetry operation – in a 3D space. Each specific set defines a unique space group. If an atom is placed on a specific position in this 3D space filled with symmetry elements, all symmetry operations are applied to this position. If the position does not coincide with any symmetry element, it is called "general position", if it coincides with one or more symmetry elements it is called a "special position." The more symmetry elements leave an atom invariant, the less "symmetrically equivalent" atoms are generated and the higher the position's local symmetry. The sets of symmetry elements of all positions reflect the possible "site symmetries" in a space group and define the "crystallographic sites." The amount of symmetrically equivalent atoms generated on a certain site is called "multiplicity." In case there are free positional parameters on a crystallographic site, as is always true for the coordinates of the general position, a specific coordinate triplet defines a "crystallographic orbit."
6 Ionic conductors with very high conductivity are commonly referred to as superionic conductors.

References

[1] Simon P, Gogotsi Y. Materials for electrochemical capacitors. Nat Mater. 2008;7:845–54.
[2] Linpo Y, Chen GZ. Redox electrode materials for supercapatteries. J Power Sources. 2016;326:604–12.
[3] Meyer DC, Leisegang T. Electrochemical storage materials: from crystallography to manufacturing technology. Berlin, Germany: De Gruyter Oldenbourg Publishing House, 2018.
[4] Nernst W. Die elektrolytische Zersetzung wässriger Lösungen. Eur J Inorg Chem. 1897;30:1547–63.
[5] Adams S, Prasado Rao R. High power lithium ion battery materials by computational design. Phys Status Solidi. 2011;208:1746–53.
[6] Bikerman J. Structure and capacity of electrical double layer. Lond Edinb Dubl Phil Mag J Sci. 1942;33:384–97.
[7] Bergmann L, Schaefer C, Kassing R. Lehrbuch der Experimentalphysik. Band 6: Festkörper, 2. Auflage ed. Berlin, Germany: Walter de Gruyter, 2005:361. ISBN: 3-11-017485-5.
[8] Beattie GW. Nernst's theory of the concentration cell. Charleston SC, USA: BiblioBazaar, 2015. ISBN: 9781343047952.
[9] Johnson Matthey Battery Systems (former Axeon © 2012). Our Guide to Batteries. Rooksley, Milton Keynes, UK: Johnson Matthey, Precedent House. 2nd edition, 2018. accessed on Jan 26th.
[10] Gupta SV. Units of measurement: past, present and future. international system of units. In: Hull R, et al., editor(s). Springer series in materials science, Vol. 122. Heidelberg, Germany: Springer Science & Business Media, 2009. ISBN: 9783642007378.
[11] Kuchling H. Taschenbuch der Physik, 11. Auflage ed. Thun and Frankfurt/Main, Germany: Verlag Harri Deutsch, 1988:635. ISBN: 3-8171-1020-0.
[12] Nernst W. Theoretical Chemistry from the Standpoint of Avogardro's Rule & Thermodynamics, 4th ed. London,UK, New York, USA: The MacMillan Company, 1904.
[13] von Helmholtz H. Über einige Gesetze der Vertheilung elektrischer Ströme in körperlichen Leitern, mit Anwendung auf die thierisch-elektrischen Versuche. Ann Phys Chem. 1853;89:353–77.
[14] Lippmann G. Beziehungen zwischen den Capillaren und elektrischen Erscheinungen. Ann Phys. 1873;225:546–61.
[15] Gouy M. Sur la constitution de la charge électrique à la surface d'un électrolyte. J Phys Theor Appl. 1910;9:457–68.
[16] Chapman DL. LI. A contribution to the theory of electrocapillarity. Lond Edinb Dubl Phil Mag J Sci. 1913;25:475–81.
[17] Stern O. The theory of the electrolytic double-layer. Z Elektrochem. 1924;30:1014–20.
[18] Freise V. Zur Theorie der diffusen Doppelschicht. Z Elektrochem Ber Bunsenges physik Chem. 1952;56:822–7.
[19] Grahame DC. The electrical double layer and the theory of electrocapillarity. Chem Rev. 1947;41:441–501.
[20] Erdey-Gruz T, Volmer M. Zur Theorie der Wasserstoff Überspannung. Z Phys Chem. 1930;150:203–13.
[21] Erdey-Gruz T, Volmer M. Zur Frage der elektrolytischen Metallüberspannung. Z Phys Chem. 1931;157:165–81.
[22] Butler JAV. The mechanism of overvoltage and its relation to the combination of hydrogen atoms at metal electrodes. Trans Faraday Soc. 1932;28:379–82.
[23] Doyle M, Fuller TF, Newman J. Modeling of galvanostatic charge and discharge of the lithium/polymer/insertion cell. J Electrochem Soc. 1993;140:1526–33.
[24] Frumkin A. Wasserstoffüberspannung und Struktur der Doppelschicht. Z Phys Chem. 1933;164:121–33.
[25] Van Soestbergen M. Frumkin-Butler-Volmer theory and mass transfer in electrochemical cells. Russ J Electrochem. 2012;48:570–9.
[26] Latz A, Zausch J. Thermodynamic derivation of a Butler–Volmer model for intercalation in Li-ion batteries. Electrochim Acta. 2013;110:358–62.

[27] Rubi J, Kjelstrup S. Mesoscopic Nonequilibrium Thermodynamics Gives the Same Thermodynamic Basis to Butler—Volmer and Nernst Equations. J Phys Chem B. 2003;107:13471–7.
[28] Zeng Y, Smith RB, Bai P, Bazant MZ. Simple formula for Marcus–Hush–Chidsey kinetics. J Electroanalytical Chem. 2014;735:77–83.
[29] Lück J, Latz A. Theory of reactions at electrified interfaces. Phys Chem Chem Phys. 2016;18:17799–804.
[30] Fick A. Über Diffusion. Annalen der Physik 170.1 (1855): 59-86. Fick A. On liquid diffusion. Phil Mag Series. 1855;4:30–9 .
[31] Hanzig J, Zschornak M, Mehner E, Hanzig F, Münchgesang W, Leisegang T, et al. The anisotropy of oxygen vacancy migration in $SrTiO_3$. J Phy Cond Matter. 2016;28:225001.
[32] Hanzig J, Zschornak M, Nentwich M, Hanzig F, Gemming S, Leisegang T, et al. Strontium titanate: an all-in-one rechargeable energy storage material. J Power Sources. 2014;267:700–5.
[33] Pearson RG. Hard and soft acids and bases, HSAB, part 1: fundamental principles. J Chem Educ. 1968;45:581–7.
[34] Wang Y, Richards WD, Ong SP, Miara LJ, Kim JC, Mo Y, et al. Design principles for solid-state lithium superionic conductors. Nat Mater. 2015;14:1026–31.
[35] Meutzner F, Münchgesang W, Kabanova NA, Zschornak M, Leisegang T, Blatov VA, et al. On the way to new possible na-ion conductors: the voronoi–dirichlet approach, data mining and symmetry considerations in ternary Na oxides. Chem Eur J. 2015;21:16601–8.
[36] Huggins RA. Chapter 9: Very Rapid Transport in Solids. In: Nowick AS, editor(s). Diffusion in solids: recent developments. New York, USA: Academic Press, 1975:445–86. ISBN: 0-12-522660-8.
[37] Neumann F. In: Meyer OE, editor(s). Vorlesungen über die Theorie der Elastizität der festen Körper und des Lichtäthers. Leipzig, Germany: B. G. Teubner-Verlag, 1885.
[38] van der Veen A, Bhattacharya J, Belak AA. Understanding Li Diffusion in Li-Intercalation Compounds. Acc Chem Res. 2013;46:1216–25.
[39] Rong Z, Malik R, Canepa P, Sai Gautam G, Liu M, Jain A, et al. Materials design rules for multivalent ion mobility in intercalation structures. Chem Mater. 2015;27:6016–21.
[40] Yakovenko AA, Wei ZW, Wriedt M, Li JR, Halder GJ, Zhou HC. Study of guest molecules in metal organic frameworks by powder X-ray diffraction: analysis of difference envelope density. Cryst Growth Des. 2014;14:5397–407.
[41] Zschornak M, Richter C, Nentwich M, Stöcker H, Gemming S, Meyer DC. Probing a crystal's short-range structure and local orbitals by Resonant X-ray Diffraction methods. Crystal Res Technol. 2014;49:43–54
[42] Richter C, Zschornak M, Novikov D, Mehner E, Nentwich M, Hanzig J, Gorfman S, Meyer DC. Picometer polar atomic displacements in strontium titanate determined by resonant X-ray diffraction. Nat Comms. 2018;9:178.
[43] Wengert S, Nesper R, Andreoni W, Parrinello M. Ionic diffusion in a ternary superconductor: an ab initio molecular dynamics study. Phys Rev Lett. 1996;77:5083–5.
[44] Shi SQ, Lu P, Liu ZY, Qi Y, Hector LG, Li H, et al. Direct calculation of li-ion transport in the solid electrolyte interphase. J Am Chem Soc. 2012;134:15476–87.
[45] Soto FA, Yan P, Engelhard MH, Marzouk A, Wang C, Xu G, et al. Tuning the solid electrolyte interphase for selective li- and na-ion storage in hard carbon. Adv Mater. 2017;29:1606860 .
[46] Maiser E. Battery packaging – technology review. AIP Conf Proc. 2014;1597:204–8.
[47] Korthauer R. Handbuch Lithium-Ionen-Batterien. Berlin/Heidelberg, Germany: Springer-Verlag, 2013. ISBN: 978-3-642-30652-5.
[48] Dunn B, Kamath H, Tarascon J-M. Electrical energy storage for the grid: a battery of choices. Science. 2011;334:928–35.
[49] Kraytsberg A, Ein-Eli Y. Higher, stronger, better? a review of 5 volt cathode materials for advanced lithium-ion batteries. Adv Ene Mat. 2012;2:922–39.
[50] Reddy TD, Linden D. Chapter 19 – 21: Nickel-Cadmium Batteries. Linden's handbook of batteries, 4th ed. New York City, USA: McGrawHill Verlag, 2011. ISBN: 978-0071624213.
[51] Page KA, Soles CL, Runt J. Polymers for energy storage and delivery: polyelectrolytes for batteries and fuel cells, Vol. 1096. Washington D.C., USA: American Chemical Society, 2012. ISBN: 9780841226319.
[52] Skyllas-Kazacos M, Chakrabarti MH, Hajimolana SA, Mjalli FS, Saleem M. Progress in flow battery research and development. J Electrochem Soc. 2011;158:R55–R79.
[53] Wang W, Luo Q, Li B, Wei X, Li L, Yang Z. Recent progress in redox flow battery research and development. Adv Funct Mater. 2013;23:970–86.
[54] Ponce De León C, Frías-Ferrer A, González-García J, Szánto DA, Walsh FC. Redox flow cells for energy conversion. J Power Sources. 2006;160:716–32.
[55] Cheng F, Chen J. Metal–air batteries: from oxygen reduction electrochemistry to cathode catalysts. Chem Soc Rev. 2012;41:2172–92.
[56] Reddy TD, Linden D. Chapter 16 & 17: Lead-Acid Batteries & Valve Regulated Lead-Acid Batteries. Linden's Handbook of Batteries, 4th ed. New York City, Vereinigte Staaten: McGrawHill Verlag, 2011. ISBN: 978-0071624213.
[57] Hahn T (Hrsg.). International tables for crystallography. Bd. A: Space-group symmetry. 5., rev. ed., repr. with corr. Dordrecht: Kluwer Academic Publishers, 2002. ISBN: 0-7923-6591-7.
[58] Atkins PW, de Paula J. Physikalische Chemie, 4. vollständig überarbeitete Auflage ed. Weinheim, Germany: Wiley-VCH Verlag, 2006. ISBN: 978-3-527-31807-0.
[59] Mortimer CE, Müller U. Chemie: Das Basiswissen der Chemie, 10. Auflage ed. Stuttgart, Germany: Georg Thieme Verlag, 2007. ISBN: 978-3134843095.
[60] Hollemann AF, Wiberg N. Lehrbuch der Anorganischen Chemie, 102. Auflage ed. Berlin, Germany: Walter de Gruyter Verlag, 2007. ISBN: 978-3110177701.
[61] Schmidt VM. Elektrochemische Verfahrenstechnik – Grundlagen, Reaktionskinetik, Prozessoptimierung. Weinheim, Germany: Wiley-VCH Verlag, 2003. ISBN: 978-3-527-29958-4.
[62] Riedel E, Janiak C. Anorganische Chemie, 7. Auflage ed. Berlin, Germany: Walter de Gruyter Verlag, 2007. ISBN: 978-3110189032.